Electroweak bremsstrahlung from neutron-neutron scattering

Yi Li,[1] M. K. Liou,[2] and W. M. Schreiber[3]

[1]*College of Physics and Technology, Guangxi University, Nanning, Guangxi 530004, People's Republic of China*

[2]*Department of Physics and Institute for Nuclear Theory, Brooklyn College of the City University of New York, Brooklyn, New York 11210, USA*

[3]*Department of Physics, College of Staten Island of the City University of New York, Staten Island, New York 10314, USA*

(Received 22 June 2009; revised manuscript received 6 August 2009; published 22 September 2009)

Background: Nucleon-nucleon (NN) bremsstrahlung processes $NN\gamma$ ($nn\gamma$, $np\gamma$, and $pp\gamma$) have been extensively investigated. Neutrino-pair bremsstrahlung processes from nucleon-nucleon scattering $NN\nu\bar{\nu}$ ($nn\nu\bar{\nu}$, $np\nu\bar{\nu}$, and $pp\nu\bar{\nu}$) have recently attracted attention in studies of neutrino emission in neutron stars. The calculated $NN\nu\bar{\nu}$ cross sections (or emissivities) are found to be sensitive to the two-nucleon dynamical model used in the calculations. **Purpose and Method**: A realistic one-boson-exchange (ROBE) model for NN interactions is used to construct the electroweak bremsstrahlung amplitudes using the well-known nucleon electromagnetic and weak interaction vertices. The constructed $nn\gamma$ and $nn\nu\bar{\nu}$ amplitudes are investigated by applying them to calculate $nn\gamma$ and $nn\nu\bar{\nu}$ cross sections, respectively. **Results**: (i) The 190-MeV ROBE $nn\gamma$ cross sections agree well with those calculated using the TuTts amplitude, but they are in disagreement with those calculated using the Low amplitude. (ii) The calculated $nn\nu\bar{\nu}$ cross sections using the ROBE amplitude at the neutrino-pair energy $\omega = 1$ MeV are in quantitative agreement with those calculated by Timmermans *et al.* [Phys. Rev. C **65**, 064007 (2002)], who used the leading-order term of the soft neutrino-pair bremsstrahlung amplitude. **Conclusions**: The $nn\gamma$ amplitude in the ROBE approach, which obeys the soft-photon theorem, has a predictive power similar to that of the TuTts amplitude. The $nn\nu\bar{\nu}$ amplitude in the ROBE approach, which is consistent with the soft neutrino-pair bremsstrahlung theorem, has a predictive power similar to that of the soft neutrino-pair bremsstrahlung amplitude of Timmermans *et al.* in the low neutrino-pair energy region.

DOI: 10.1103/PhysRevC.80.035505 PACS number(s): 12.15.Ji, 13.75.Cs, 24.80.+y, 26.60.−c

I. INTRODUCTION AND $nn\gamma$ RESULTS

Recent studies of neutrino emission processes in neutron stars have focused on the neutrino-pair bremsstrahlung from nucleon-nucleon scattering [1–4]. Two processes that have received particular attention are

$$n + n \rightarrow n + n + \nu + \bar{\nu}, \quad (1)$$

$$n + p \rightarrow n + p + \nu + \bar{\nu}, \quad (2)$$

which we will denote as the $nn\nu\bar{\nu}$ and $np\nu\bar{\nu}$ processes, respectively. One of the main purposes of these new studies is to understand quantitatively the effect of the nucleon-nucleon interaction on the neutrino-pair bremsstrahlung cross section (or the neutrino emissivity) for the $nn\nu\bar{\nu}$ and $np\nu\bar{\nu}$ processes. These studies have clearly demonstrated that the calculated cross sections or emissivities depend sensitively on the two-nucleon dynamical model used in the calculations. A most important finding is that predicted cross sections or emissivities calculated using realistic two-nucleon models are roughly a factor of 4–5 below the results based on the simple one-pion-exchange (OPE) model in higher neutron incident momentum regions. The emissivities for the $nn\nu\bar{\nu}$ and $np\nu\bar{\nu}$ processes were first calculated using the OPE model by Friman and Maxwell [5]. The results of the new calculations are qualitatively similar, but some discrepancies still exist. To thoroughly understand the $nn\nu\bar{\nu}$ and $np\nu\bar{\nu}$ processes, the discrepancies must be resolved. It is especially important to know whether all these calculations yield quantitatively similar $nn\nu\bar{\nu}$ and/or $np\nu\bar{\nu}$ cross sections in free space. Moreover, other approaches should also be used to investigate these processes.

We have developed a realistic one-boson-exchange (ROBE) approach to investigate the electroweak bremsstrahlung processes, which include processes involving photon bremsstrahlung from nucleon-nucleon scattering $NN\gamma$ ($nn\gamma$, $np\gamma$, and $pp\gamma$) and processes involving neutrino-pair bremsstrahlung from nucleon-nucleon scattering $NN\nu\bar{\nu}$ ($nn\nu\bar{\nu}$, $np\nu\bar{\nu}$, and $pp\nu\bar{\nu}$). The photon bremsstrahlung ($NN\gamma$) amplitudes in the ROBE approach obey the soft-photon theorem [6,7], and the neutrino-pair bremsstrahlung ($NN\nu\bar{\nu}$) amplitudes in the ROBE approach are consistent with the soft neutrino-pair bremsstrahlung theorem [1]. Both the $NN\gamma$ and $NN\nu\bar{\nu}$ amplitudes are generated from Horowitz's OBE [8] model for the two-nucleon interaction. As discussed in previous papers [9,10], the Horowitz OBE model is an alternative representation of the two-nucleon elastic amplitude. It involves a set of OBE parameters (masses, complex coupling constants, and cutoff parameters) that have been determined by fitting to the Arndt amplitudes directly without iteration of the meson exchanges. The main difference between the standard Goldberger-Grisaru-MacDowell-Wong (GGMW) amplitude [11] and the Horowitz OBE amplitude is that the GGMW amplitude is expressed in terms of a set of phase shifts whereas the Horowitz amplitude is expressed in terms of a set of OBE parameters. The GGMW amplitude has been used as an input for all nucleon-nucleon bremsstrahlung calculations using the two-u-two-t special (TuTts) amplitude in the soft-photon approach [12–17].

The photon bremsstrahlung amplitudes in the ROBE approach have already been successfully applied to describe both $pp\gamma$ and $np\gamma$ processes [9,10,18,19]. We emphasize that these

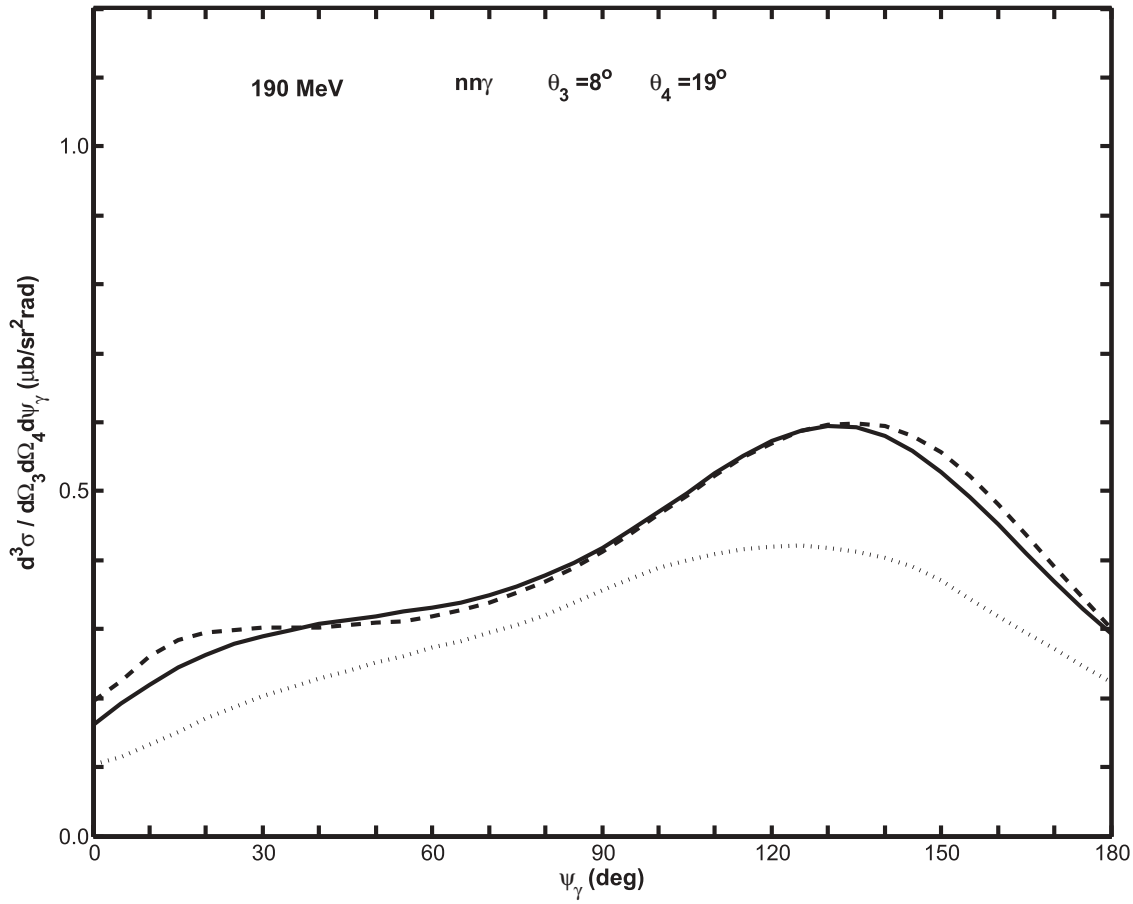

FIG. 1. Coplanar $nn\gamma$ cross sections at 190 MeV for $(\theta_3,\theta_4) = (8^\circ,19^\circ)$. The solid curve is the result obtained from the ROBE model. The dashed and dotted curves correspond to soft-photon results obtained from the TuTts amplitude and the Low amplitude, respectively [12].

photon bremsstrahlung amplitudes and the TuTts amplitudes predict quantitatively similar $pp\gamma$ and $np\gamma$ cross sections, and the predicted cross sections are in excellent agreement with the experimentally measured cross sections for most cases. The quantitative agreement observed between the high-precision Kernfysisch-Versneller-Instituut (KVI) $pp\gamma$ cross section data and the theoretical predictions calculated using both the $pp\gamma$ amplitude in the ROBE approach and the TuTts $pp\gamma$ amplitude in the soft-photon approach is an excellent example [10]. To demonstrate that such a quantitative agreement can also be found in the $nn\gamma$ process, we have applied the $nn\gamma$ amplitude in the ROBE approach to calculate the $nn\gamma$ cross sections at 190 MeV for $(\theta_3, \theta_4) = (8^\circ, 19^\circ)$. The results are compared with those calculated using both the Low $nn\gamma$ amplitude and the TuTts $nn\gamma$ amplitude in the soft-photon approach [12]. As shown in Fig. 1, the agreement between the results calculated from the $nn\gamma$ amplitude in the ROBE approach (pseudoscalar coupling) and the TuTts $nn\gamma$ amplitude in the soft-photon approach is indeed excellent in the kinematic region investigated. As discussed in Refs. [13,14] (appendix), the primary difference between the Low amplitude and the TuTts amplitude lies in the very different on-shell kinematic points at which the two amplitudes are evaluated. The TuTts amplitude depends upon four different on-shell points (one for each bremsstrahlung emission process), whereas the Low amplitude utilizes a unique common (average) on-shell point for all four emission processes. For the $pp\gamma$ and $nn\gamma$ processes, an important advantage for the TuTts amplitudes is that they retain most of the important contributions from all κ-dependent terms (where κ = the anomalous magnetic moment κ_p or κ_n). (For the $np\gamma$ process, the Low, TuTts, and ROBE amplitudes predict very similar $np\gamma$ cross sections.) The ROBE $NN\gamma$ amplitudes have very similar predictive power to the TuTts $NN\gamma$ amplitudes, mainly because the ROBE $NN\gamma$ amplitudes also depend on four different on-shell points and include all κ-dependent terms. Further discussion on this matter is contained in the following section.

We have also successfully applied one of the neutrino-pair bremsstrahlung amplitudes in the ROBE approach to calculate the $nn\nu\bar{\nu}$ cross sections. The most interesting result obtained from our calculations is that the calculated cross sections at $\omega = 1$ MeV (the neutrino-pair energy) are quantitatively similar to those obtained by Timmermans *et al.* using a soft neutrino-pair bremsstrahlung amplitude [1]. Thus we have found that our photon bremsstrahlung amplitudes have very similar predictive power to the TuTts amplitude in the soft-photon approach, and our neutrino-pair bremsstrahlung amplitude for the $nn\nu\bar{\nu}$ process has very similar predictive power to the soft neutrino-pair bremsstrahlung amplitude of Timmermans *et al.* The primary purpose of this paper is to

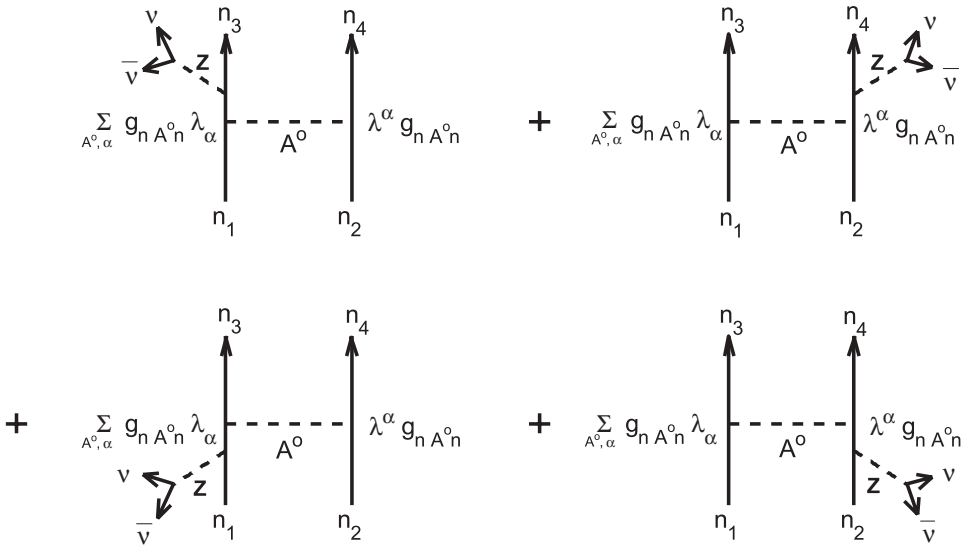

FIG. 2. Diagrams for the $nn\nu\bar{\nu}$ process.

present the expression for the $nn\nu\bar{\nu}$ amplitude in the ROBE approach used in our $nn\nu\bar{\nu}$ calculations, to show the calculated $nn\gamma$ cross sections and $nn\nu\bar{\nu}$ cross sections, and to compare our results with other predictions calculated using different approaches.

II. $nn\nu\bar{\nu}$ AMPLITUDE

The relevant diagrams for the $nn\nu\bar{\nu}$ process are shown in Fig. 2. In these diagrams, A^0 represents 10 different neutral mesons (π^0, ρ^0, δ^0, t_1^0, a_1^0, η, σ, ω, t_0, and a_0) that can be exchanged between two neutrons, g_{nA^0n} represents the coupling constant mediating the coupling of the meson A^0 to the nn current, and λ^α ($\alpha = 1, 2, 3, 4, 5$) represents the 5 Fermi covariants. Other factors are suppressed. The Z-boson propagator, which is attached to both the nucleon vertex and to the neutrino-pair vertex, can be simplified as follows:

$$-i\frac{g_{\mu\nu} - q_\mu q_\nu/M_Z^2}{q^2 - M_Z^2} \approx i\frac{1}{M_Z^2}g_{\mu\nu} \tag{3}$$

for the neutrino-pair energy region considered here. In the c.m. frame, the expression for the cross section $\frac{d\sigma}{d\omega}$ is given by (see, e.g., Ref. [1])

$$\begin{aligned}\frac{d\sigma}{d\omega} &= 3\times\frac{m^4}{2\sqrt{s(s-4m^2)}(2\pi)^8}\frac{16\pi}{3}\frac{G_F^2}{2}\frac{|\vec{p}_3|}{\sqrt{s}-\omega}\\ &\times\frac{1}{4}\sum_{\text{neutron spins}}\int\!\!\int (M_\mu q^\mu M_\rho^* q^\rho - q^2 M^\mu M_\mu^*)\\ &\times d\Omega(\vec{p}_3)d^3\vec{q},\end{aligned} \tag{4}$$

where m is the nucleon mass, $\vec{p}_3$ is the outgoing neutron c.m. momentum, $q^\mu = (\omega,\vec{q})$ is the neutrino-pair four-momentum, $s = 4(m^2 + \vec{p}^{\,2})$, $\vec{p}$ is the incident neutron momentum in the c.m. frame, and the Fermi weak interaction constant $G_F = 1.166\times10^{-5}$ GeV^{-2}.[1] (The Bjorken-Drell convention for the metric and the γ matrices is used in our work.) The factor of 3 corresponds to the emission of three neutrino-pair flavors.

The amplitude M^μ has the form

$$\begin{aligned}M^\mu &\equiv M^\mu(t_{13}, t_{24}, u_{14}, u_{23})\\ &= \sum_{A^0,\alpha}\left\{\left[\frac{F_{A^0}(t_{24})}{(p_3+q)^2-m^2}\bar{u}(p_3)\Gamma^\mu(\not{p}_3+\not{q}+m)\right.\right.\\ &\times g_{nA^0n}\lambda^\alpha u(p_1)\bar{\mathbf{u}}(p_4)g_{nA^0n}\lambda_\alpha u(p_2)\\ &+\frac{F_{A^0}(t_{13})}{(p_4+q)^2-m^2}\bar{u}(p_3)g_{nA^0n}\lambda^\alpha\\ &\times u(p_1)\bar{\mathbf{u}}(p_4)\Gamma^\mu(\not{p}_4+\not{q}+m)g_{nA^0n}\lambda_\alpha u(p_2)\\ &+\frac{F_{A^0}(t_{24})}{(p_1-q)^2-m^2}\bar{u}(p_3)g_{nA^0n}\lambda^\alpha(\not{p}_1-\not{q}+m)\Gamma^\mu\\ &\times u(p_1)\bar{\mathbf{u}}(p_4)g_{nA^0n}\lambda_\alpha u(p_2)\\ &+\frac{F_{A^0}(t_{13})}{(p_2-q)^2-m^2}\bar{u}(p_3)g_{nA^0n}\lambda^\alpha\\ &\left.\left.\times u(p_1)\bar{\mathbf{u}}(p_4)g_{nA^0n}\lambda_\alpha(\not{p}_2-\not{q}+m)\Gamma^\mu u(p_2)\right]\right.\\ &\left.-\text{terms}\,(p_3\Leftrightarrow p_4, t_{13}\to u_{14}, t_{24}\to u_{23})\right\}.\end{aligned} \tag{5}$$

In Eq. (5), $t_{ij} = (p_i - p_j)^2$ ($ij = 13, 24$) and $u_{ik} = (p_i - p_k)^2$ ($ik = 14, 23$) are Mandelstam variables, $F_{A^0}(t_{ij})$ [$F_{A^0}(u_{ik})$] represent the other relevant factors (defined in terms of t_{ij} and u_{ik}, the mass of the exchanged meson m_{A^0} and the

[1] For the approximation indicated in Eq. (3) and a coupling of $\frac{g}{2\cos\theta_w}$ at each vertex, one has $\frac{g^2}{4M_Z^2\cos^2\theta_w} = \frac{g^2}{4M_w^2} = \frac{2G_F}{\sqrt{2}}$.

cutoff parameters Λ_{A^0}),

$$F_{A^0}(t_{ij}) = \frac{-4\pi}{t_{ij} - m_{A^0}^2} \frac{1}{\left(1 - t_{ij}/\Lambda_{A^0}^2\right)^2} \quad (ij = 13, 24), \tag{6a}$$

$$F_{A^0}(u_{ik}) = F_{A^0}(t_{ij} \to u_{ik}, ij = 13, 24 \to ik = 14, 23), \tag{6b}$$

and the weak interaction nucleon vertex function Γ^μ is[2]

$$\Gamma^\mu = \frac{1}{2}\left(F_1^V + 2F_1^n \sin^2\theta_w\right)\gamma^\mu + \frac{1}{2}G_A\gamma^\mu\gamma^5 - \frac{i}{2}\left(F_2^V + 2F_2^n \sin^2\theta_w\right)\sigma^{\mu\rho}q_\rho. \tag{7}$$

In Eq. (7), we set $F_1^V = 1$, $F_1^n = 0$, $G_A = -1.257$, $F_2^V = \frac{\kappa_p - \kappa_n}{2m}$, $F_2^n = \frac{\kappa_n}{2m}$, the respective nucleon anomalous magnetic moments $\kappa_p = 1.793$ and $\kappa_n = -1.913$, and $\sin^2\theta_w = 0.234$ for the Weinberg angle θ_w. We note that for the corresponding $pp\nu\bar{\nu}$ process $F_{1,2}^n$ are replaced by $-F_{1,2}^p$ in this expression for Γ^μ, where $F_1^p = 1$ and $F_2^p = \frac{\kappa_p}{m}$. It is clear that M^μ, which depends on $(t_{13}, t_{24}, u_{14}, u_{23})$, is a two-u-two-t type amplitude. In other words, $M^\mu(t_{13}, t_{24}, u_{14}, u_{23})$ is evaluated at four different on-shell points whose respective conditions are

$$s_{21} + u_{23} + t_{13} = 4m^2, \tag{8a}$$

$$s_{22} + u_{23} + t_{24} = 4m^2, \tag{8b}$$

$$s_{12} + u_{14} + t_{24} = 4m^2, \tag{8c}$$

$$s_{11} + u_{14} + t_{13} = 4m^2, \tag{8d}$$

where

$$\begin{aligned} s_{21} &= s_i - 2p_4 \cdot q, \\ s_{12} &= s_i - 2p_3 \cdot q, \\ s_{22} &= s_f + 2p_1 \cdot q, \\ s_{11} &= s_f + 2p_2 \cdot q, \\ s_i &= (p_1 + p_2)^2, \\ s_f &= (p_3 + p_4)^2. \end{aligned} \tag{9}$$

From the amplitude M^μ given by Eq. (5), we can define a leading amplitude $\tilde{M}^\mu$ by keeping only the leading-order term (in q) of M^μ:

$$\begin{aligned} \tilde{M}^\mu &\equiv \tilde{M}^\mu(t_{13}, t_{24}, u_{14}, u_{23}) \\ &= \sum_{A^0,\alpha} \left\{ \left[\frac{F_{A^0}(t_{24})}{2p_3 \cdot q} \bar{u}(p_3)\tilde{\Gamma}^\mu(\not{p}_3 + m) \right.\right. \\ &\quad \times g_{nA^0n}\lambda^\alpha u(p_1)\bar{u}(p_4)g_{nA^0n}\lambda_\alpha u(p_2) \\ &\quad + \frac{F_{A^0}(t_{13})}{2p_4 \cdot q} \bar{u}(p_3)g_{nA^0n}\lambda^\alpha u(p_1)\bar{u}(p_4)\tilde{\Gamma}^\mu \\ &\quad \times (\not{p}_4 + m)g_{nA^0n}\lambda_\alpha u(p_2) \\ &\quad - \frac{F_{A^0}(t_{24})}{2p_1 \cdot q} \bar{u}(p_3)g_{nA^0n}\lambda^\alpha(\not{p}_1 + m)\tilde{\Gamma}^\mu u(p_1) \\ &\quad \times \bar{u}(p_4)g_{nA^0n}\lambda_\alpha u(p_2) \\ &\quad - \frac{F_{A^0}(t_{13})}{2p_2 \cdot q} \bar{u}(p_3)g_{nA^0n}\lambda^\alpha u(p_1) \\ &\quad \left.\left. \times \bar{u}(p_4)g_{nA^0n}\lambda_\alpha(\not{p}_2 + m)\tilde{\Gamma}^\mu u(p_2) \right] \right. \\ &\quad \left. - \text{terms}\,(p_3 \Leftrightarrow p_4, t_{13} \to u_{14}, t_{24} \to u_{23}) \right\}, \end{aligned} \tag{10}$$

where

$$\tilde{\Gamma}^\mu = \tfrac{1}{2}\left(F_1^V + 2F_1^n \sin^2\theta_w\right)\gamma^\mu + \tfrac{1}{2}G_A\gamma^\mu\gamma^5. \tag{11}$$

If we expand the amplitude $\tilde{M}^\mu$ about the average $\bar{t}$ [$\bar{t} = \frac{1}{2}(t_{13} + t_{24})$] and the average $\bar{u}$ [$\bar{u} = \frac{1}{2}(u_{14} + u_{23})$], then we obtain another leading amplitude $\bar{M}^\mu(\bar{t},\bar{u})$,

$$\begin{aligned} \bar{M}^\mu &\equiv \bar{M}^\mu(\bar{t}, \bar{u}) \\ &= \tilde{M}^\mu(t_{13} \to \bar{t}, t_{24} \to \bar{t}, u_{14} \to \bar{u}, u_{23} \to \bar{u}). \end{aligned} \tag{12}$$

Thus, it is clear that $\bar{M}^\mu(\bar{t}, \bar{u})$ is evaluated at a unique on-shell point satisfying the condition

$$\bar{s} + \bar{u} + \bar{t} = 4m^2, \tag{13}$$

where

$$\bar{s} = \tfrac{1}{2}(s_i + s_f). \tag{14}$$

III. $nn\nu\bar{\nu}$ RESULTS AND DISCUSSION

Equation (4) has been used to calculate the cross section $\frac{d\sigma}{d\omega}$ for the $nn\nu\bar{\nu}$ process in free space. The cross sections $\frac{d\sigma}{d\omega}$ as a function of the incident neutron momentum p at three neutrino-pair energies ($\omega = 0.5$, 1, and 2 MeV) are shown in Fig. 3. In Fig. 3(b), our result at $\omega = 1$ MeV is compared with that obtained by Timmermans *et al.* [1]. It is clear that the two results are in quantitative agreement with each other throughout the entire momentum region. The fact that two completely independent calculations based on two different approaches can yield such excellent agreement is extremely interesting and important. To understand the reason for the quantitative agreement observed in Fig. 3(b), the following investigations have been made:

(i) Timmermans *et al.* employed a leading-order term of the soft neutrino-pair bremsstrahlung amplitude (derived from the soft electroweak bremsstrahlung theorem [1]) to calculate the $nn\nu\bar{\nu}$ cross sections. We use a neutrino-pair bremsstrahlung amplitude [Eq. (5)] developed from the ROBE approach, which includes not only the leading-order term (equivalent to the amplitude used by Timmermans *et al.*[3]) but also higher order terms. In an attempt to estimate the effect of the higher order terms on the $nn\nu\bar{\nu}$ cross sections, we have used the leading amplitude $\tilde{M}^\mu$ [Eq. (10)] to calculate the cross

[2] A pseudoscalar term $-i\frac{1}{2}G_p q^\mu\gamma^5$ is omitted from the Γ^μ expression, since it yields an identically zero contribution in Eq. (4).

[3] This leading-order term includes the vector current amplitude and the axial-current amplitude. For obtaining the vector current amplitude, the relations $\bar{u}(p)\gamma^\mu(\not{p} + m) = \bar{u}(p)2p^\mu$ and $(\not{p} + m)\gamma^\mu\bar{u}(p) = 2p^\mu\bar{u}(p)$ are useful.

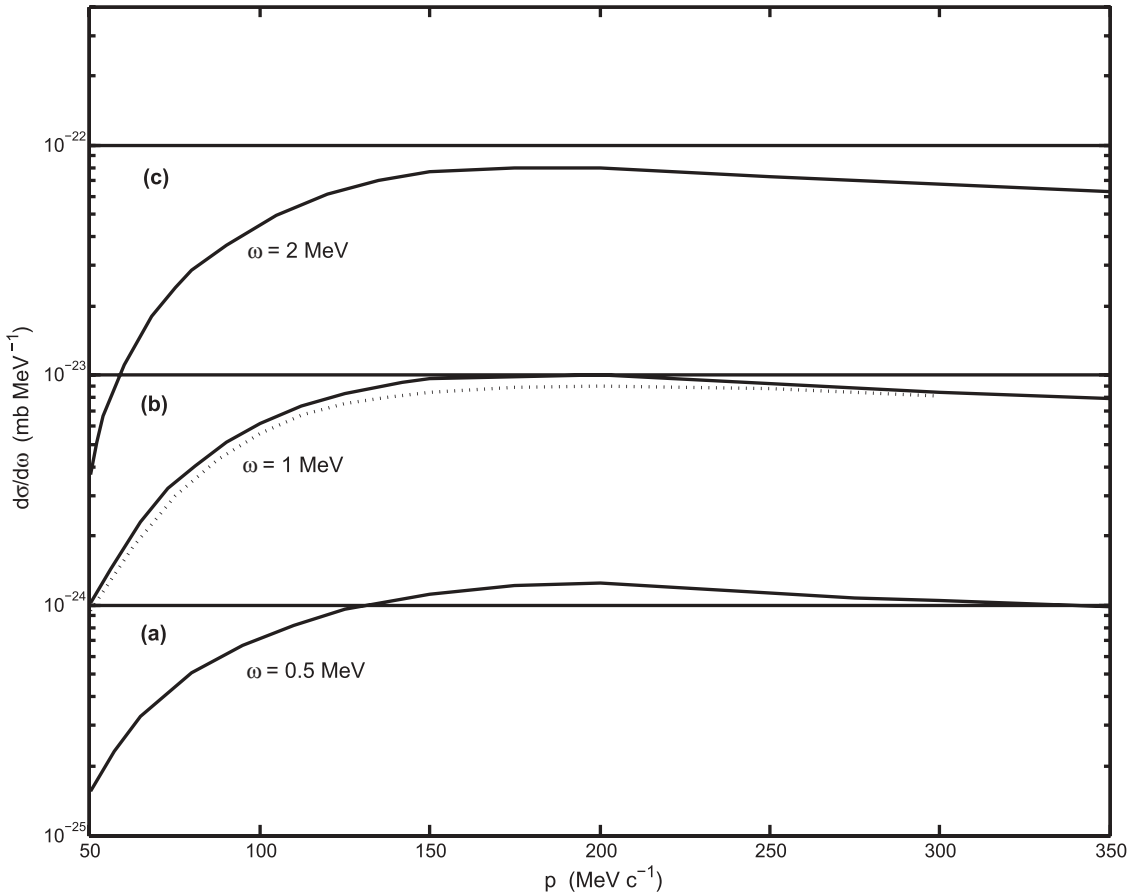

FIG. 3. The cross section $\frac{d\sigma}{d\omega}$ as a function of the incident neutron momentum p, corresponding to neutrino-pair energies ω of (a) 0.5, (b) 1, and (c) 2 MeV, respectively. All solid curves represent results obtained from the ROBE model. The dotted curve shown in Fig. 3(b) is the soft neutrino-pair bremsstrahlung result obtained in Ref. [1].

sections at $\omega = 1$ MeV. We have found that the cross sections calculated using the amplitude $\tilde{M}^{\mu}$ are extremely close to those calculated using the complete amplitude M^{μ} (with the difference, on the average, being about 0.1%). Thus the quantitative agreement between our calculations and the calculations of Timmermans *et al.* is because the contribution from the higher order terms is negligible for the case of low neutrino-pair energy ω. Most importantly, the agreement implies that our $nn\nu\bar{\nu}$ amplitude is consistent with the soft electroweak (neutrino-pair) bremsstrahlung theorem and also that both the amplitude of Timmermans and our amplitude are valid and can be used to describe the $nn\nu\bar{\nu}$ process at low-energy ω.

(ii) We should point out that the soft $nn\nu\bar{\nu}$ amplitude derived by Timmermans *et al.* is basically a one-on-shell-point model [because the amplitude is evaluated at a common (average) on-shell kinematic point]. It is, therefore, different from our ROBE $nn\nu\bar{\nu}$ amplitude, which is a four-on-shell-point model (i.e., the amplitude depends on four different on-shell kinematic points). This explains why our leading-order amplitude $\tilde{M}^{\mu}$ is not exactly the same as the leading-order amplitude of Timmermans *et al.* This can also be seen from the small difference in the cross section between the solid curve (our amplitude) and the dotted curve (the amplitude of Timmermans *et al.*) shown in Fig. 3(b). We have found that this small difference between the solid curve and the dotted curve is partially because the two amplitudes are evaluated at different on-shell points. More precisely, we have investigated the effect of the different on-shell-point conditions on the cross section $\frac{d\sigma}{d\omega}$ to understand the difference between the solid curve and the dotted curve. To do this, we have expanded our amplitude $\tilde{M}^{\mu}$ about the average on-shell kinematic point $(\bar{t},\bar{u})$ to obtain a new leading-order $nn\nu\bar{\nu}$ amplitude $\bar{M}^{\mu}(\bar{t},\bar{u})$ [Eq. (12)], which is evaluated at the same on-shell point $(\bar{t},\bar{u})$ used by Timmermans *et al.* This new amplitude $\bar{M}^{\mu}$ has been applied to calculate the $nn\nu\bar{\nu}$ cross section at $\omega = 1$ MeV. As an example, we use the point $p = 250$ MeV/c to discuss our result. From Fig. 3(b), at $p = 250$ MeV/c the difference in the cross sections between the solid curve (calculated using our full ROBE amplitude M^{μ}) and the dotted curve is about 12.9%. The new amplitude $\bar{M}^{\mu}$ reduces the difference from 12.9% to about 4.8%, which is closer to the result of Timmermans *et al.* Thus, the different on-shell-point conditions

do affect the cross section $\frac{d\sigma}{d\omega}$ even at the very low neutrino-pair energy $\omega = 1$ MeV. From the fact that the four-on-shell-point amplitudes are required to describe the $pp\gamma$ data [12,13], we expect that the four-on-shell-point amplitudes would also be needed to describe the $nn\nu\bar{\nu}$ process in the energy region with higher incident neutron energies and higher neutrino-pair energies.

(iii) We have studied the appropriate elastic input parameters that should be used in our calculation of the three cross section curves shown in Fig. 3. The original Horowitz parameters have been used to calculate cross sections for $135 \leqslant p \leqslant 350$ MeV/c. Both the Horowitz parameters at 135 MeV and new parameters (obtained by fitting to the 14.1-MeV np data) have been used to calculate cross sections for $50 \leqslant p \leqslant 135$ MeV/c. Our investigations revealed that these calculated cross sections were insensitive to which set of parameters were used.

IV. CONCLUSION

In conclusion, we have developed the electroweak bremsstrahlung amplitudes in the ROBE approach, which include photon bremsstrahlung amplitudes for $NN\gamma$ processes and the neutrino-pair bremsstrahlung amplitudes for $NN\nu\bar{\nu}$ processes. The photon bremsstrahlung amplitudes obey the soft-photon theorem, whereas the neutrino-pair bremsstrahlung amplitudes are consistent with the soft neutrino-pair bremsstrahlung theorem. Our investigations reveal that the $NN\gamma$ amplitudes in the ROBE approach have very similar predictive power to the TuTts amplitudes in the soft-photon approach. Because the $pp\gamma$ and $np\gamma$ amplitudes in both approaches have already been successfully applied to describe the $pp\gamma$ and $np\gamma$ processes, respectively, we expect that the $nn\gamma$ amplitudes in both approaches should be able to describe the $nn\gamma$ process. We have also observed that the $nn\nu\bar{\nu}$ amplitude in the ROBE approach has very similar predictive power to the $nn\nu\bar{\nu}$ amplitude derived from the soft neutrino-pair bremsstrahlung theorem by Timmermans *et al.* There is quantitative agreement between the two calculations in the neutrino-pair low-energy region, and this comparative method can be used quite generally. Furthermore, by virtue of its diagrammatic formalism, the ROBE approach can readily be extended to other energy regions, as well as to other relevant emission processes in nucleon-nucleon scattering.

ACKNOWLEDGMENTS

We thank Xiaoyin Pan for his assistance in obtaining the 14.1-MeV Horowitz parameters. M. K. Liou thanks R. G. E. Timmermans for the $nn\gamma$ cross section results presented in Fig. 1. The work of Yi Li was supported by a grant from Guangxi University, and the work of M. K. Liou and W. M. Schreiber was supported in part by the CUNY Professional Staff Congress-Board of Higher Education Research Award Program.

[1] R. G. E. Timmermans, A. Yu. Korchin, E. N. E. van Dalen, and A. E. L. Dieperink, Phys. Rev. C **65**, 064007 (2002).
[2] E. N. E. van Dalen, A. E. L. Dieperink, and J. A. Tjon, Phys. Rev. C **67**, 065807 (2003).
[3] C. Hanhart, D. R. Phillips, and S. Reddy, Phys. Lett. **B499**, 9 (2001).
[4] S. Stoica, V. P. Paun, and A. G. Negoita, Phys. Rev. C **69**, 068801 (2004).
[5] B. L. Friman and O. V. Maxwell, Astrophys. J. **232**, 541 (1979).
[6] F. E. Low, Phys. Rev. **110**, 974 (1958).
[7] S. L. Adler and Y. Dothan, Phys. Rev. **151**, 1267 (1966).
[8] C. J. Horowitz, Phys. Rev. C **31**, 1340 (1985).
[9] M. K. Liou, Y. Li, W. M. Schreiber, and R. W. Brown, Phys. Rev. C **52**, R2346 (1995); Y. Li, M. K. Liou, and W. M. Schreiber, *ibid.* **57**, 507 (1998).
[10] Y. Li, M. K. Liou, and W. M. Schreiber, Phys. Rev. C **72**, 024005 (2005).
[11] M. L. Goldberger, M. T. Grisaru, S. W. MacDowell, and D. Y. Wong, Phys. Rev. **120**, 2250 (1960).
[12] R. G. E. Timmermans, T. D. Penninga, B. F. Gibson, and M. K. Liou, Phys. Rev. C **73**, 034006 (2006).
[13] M. K. Liou, T. D. Penninga, R. G. E. Timmermans, and B. F. Gibson, Phys. Rev. C **69**, 011001(R) (2004).
[14] R. G. E. Timmermans, B. F. Gibson, Y. Li, and M. K. Liou, Phys. Rev. C **65**, 014001 (2001).
[15] Y. Li, M. K. Liou, R. G. E. Timmermans, and B. F. Gibson, Phys. Rev. C **58**, R1880 (1998).
[16] M. K. Liou, R. G. E. Timmermans, and B. F. Gibson, Phys. Rev. C **54**, 1574 (1996).
[17] M. K. Liou, R. G. E. Timmermans, and B. F. Gibson, Phys. Lett. **B345**, 372 (1995); **B355**, 606(E) (1995).
[18] Y. Li, M. K. Liou, and W. M. Schreiber, Phys. Rev. C **64**, 064002 (2001).
[19] Y. Li, M. K. Liou, W. M. Schreiber, B. F. Gibson, and R. G. E. Timmermans, Phys. Rev. C **77**, 044001 (2008).